High-power terahertz quantum-cascade lasers

B.S. Williams, S. Kumar, Q. Hu and J.L. Reno

Demonstration of quantum-cascade lasers at ~4.4 THz ($\lambda \sim 68$ µm), which are measured to emit 248 mW peak power in pulsed mode, and 138 mW continuous-wave power at heatsink temperatures of 10 K, is reported. These lasers are based on a resonant-phonon depopulation scheme, and use a semi-insulating surface-plasmon waveguide.

Introduction: Terahertz quantum-cascade lasers (QCLs) have now been demonstrated at frequencies of 1.9–5.0 THz ($\lambda \sim 60$–160 µm) [1–3], and are important additions as compact, coherent sources in a spectral region that has long lacked convenient and efficient sources. In particular, these continuous-wave (CW) lasers are well suited for use as local oscillators (LO) in heterodyne receivers [4, 5]; this is significant because harmonic multipliers, commonly used as LO sources above 300 GHz, cannot deliver more than microwatt power above 2 THz. Molecular gas lasers are also used to provide tens of milliwatts of CW power at various fixed frequencies sprinkled throughout the terahertz region, but they are somewhat large and unwieldy and require some effort to maintain their stability. While single-pixel heterodyne systems do not require much more than a milliwatt of terahertz LO power, imaging or spectroscopy applications that involve illuminating many pixels, or that require significant material penetration or travel through air would benefit tremendously from much higher power terahertz sources. Resonant-phonon terahertz QCLs have recently been demonstrated up to temperatures of 164 K in pulsed mode and 117 K in CW mode [6] with the use of 'metal–metal' waveguides. Because of their subwavelength size in the transverse and lateral dimensions, these waveguides tend to have large facet reflectivities (0.7–0.9, depending on the dimensions relative to the wavelength [7]), which leads to relatively low output powers (<10 mW). The terahertz QCLs which have displayed the largest peak output powers (~90 mW) have been based on bound-to-continuum active region designs, and have used semi-insulating (SI) surface-plasmon waveguides [8, 9], which are characterised by a larger transverse mode profile (confinement factor $\Gamma \sim 0.1$–0.5) and do not appear to exhibit enhanced facet reflectivity [7]. In this Letter, we report the demonstration of terahertz QCLs which emit 248 mW peak power in pulsed operation at ~4.4 THz, and up to 138 mW of power in CW operation.

Design and fabrication: The lasers described in this Letter are based upon the resonant-phonon active region design, in which a combination of resonant tunnelling and fast longitudinal-optical phonon scattering selectively depopulates the lower radiative state [10]. The active region design is similar to that described in [6] which lased at 2.9 THz. The thicknesses of the eight layers in a module are (with the barriers in bold) **48**/82/**17**/68/**40**/164/**34**/90 in Å and the 164 Å well is bulk doped with Si at 1.9×10^{16} cm^{-3}. Along with some modifications to the injector, the major change was to thin the 25 Å radiative barrier to 17 Å, which increased the energy separation (anticrossing) between the two radiative states to obtain a larger photon energy (calculated as 19.0 meV). This laser was intended to emit near the neutral oxygen line at 4.7 THz, which is the primary coolant of interstellar dust and therefore of great interest to the astrophysics community.

The structure, labelled FL183R-2 (EA1229), was grown in the $GaAs/Al_{0.15}Ga_{0.85}As$ material system by molecular beam epitaxy with 183 cascaded modules. The wafer was processed into SI-surface-plasmon waveguide ridge structures as described in [10], with the exception that the heavily doped layer under the active region was 0.4 µm thick and doped at $n = 3 \times 10^{18}$ cm^{-3}, and the ridges were dry etched to obtain nearly vertical sidewalls. An undoped 100 nm $Al_{0.55}Ga_{0.45}As$ etch-stop layer was grown underneath the doped contact to allow the option of metal–metal waveguide processing. Finally, the devices were lapped to a substrate thickness of ~170 µm, ridges were cleaved, and an $Al_2O_3/Ti/Au/Al_2O_3$ high-reflectivity (HR) coating was evaporated on the rear facet of selected devices. The mode was calculated using a one-dimensional Drude model solver (Fig. 1), which gave a value of $\alpha_w = 3.9$ cm^{-1} for the waveguide loss and a confinement factor of $\Gamma = 0.26$. A two-dimensional finite-element solver gave similar values of $\alpha_w = 3.0$ cm^{-1} and $\Gamma = 0.21$ for the fundamental mode in a 200 µm-wide ridge [7].

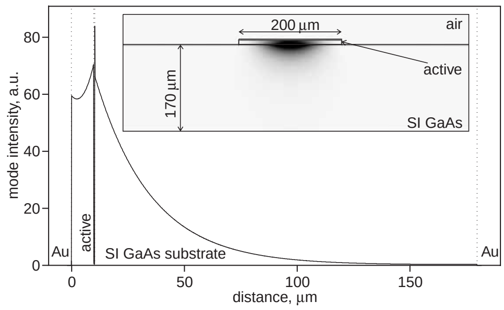

Fig. 1 *Calculated one-dimensional transverse mode profile*

Inset: Calculated two-dimensional fundamental mode intensity

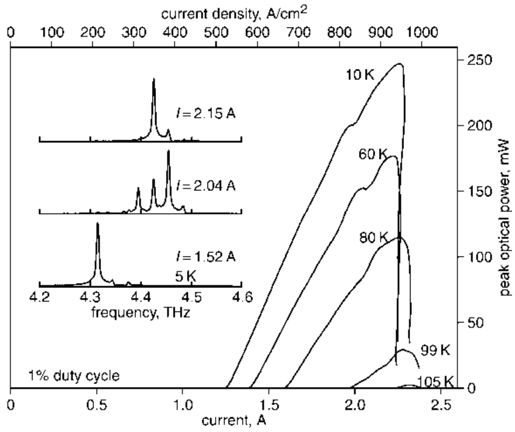

Fig. 2 *Collected pulsed light against current characteristics at various temperatures measured from 198 µm-wide, 1.21 mm-long ridge with rear facet HR coated*

Inset: Typical spectra

Results: A 198 µm-wide, 1.21 mm-long, HR-coated ridge was mounted in a vacuum cryostat and a Winston cone was used to collect light from the laser facet and bring it to the polypropylene Dewar window. The device was biased with pulse trains of 200 ns pulses repeated at 100 kHz, modulated by a 1 kHz square wave for an overall duty cycle of 1%. The output power was measured with a pyroelectric detector, with the peak level calibrated by a thermopile power meter (ScienTech model AC2500H). The collected peak output power against current is shown in Fig. 2, along with several typical spectra. At 5 K, $J_{th} = 530$ A/cm^2 in pulsed mode with a maximum peak power of 248 mW, and lasing was observed up to 105 K. Because of the large power dissipation in this device, the maximum power observed in CW operation was reduced to 138 mW, and lasing ceased at a heatsink temperature of 35 K. Somewhat more efficient CW performance was obtained from a 98 µm-wide, 2.15 mm-long HR coated structure, as the narrower ridge provided a more efficient geometry for heat removal (see Fig. 3). A maximum CW power of 123 mW was collected at 10 K (wall-plug efficiency ~0.5%) compared to a peak pulsed power of 135 mW, and lasing continued up to a maximum temperature of 40 K. The slightly higher CW operating temperature is significant for practical applications. Using a closed-cycle pulsed tube cryocooler with a few watts of cooling power at 30 K (Cryomech PT60), this laser produces ~50 mW of power, which is essential for real-time imaging using focal-plane array cameras [11]. Although J_{th} in these devices is significantly larger than in bound-to-continuum QCLs [9], these devices also have a large dynamic current range of ~400–500 A/cm^2 above threshold, which results in large output powers.

In pulsed mode, the slope efficiency was measured to be $dL/dI = 300$ mW/A, or a value of ~340 mW/A after accounting for the 85–90% transmission of the Dewar window. This is equivalent to a differential quantum efficiency (DQE) of approximately 18 photons per injected electron. The DQE is more than a factor of three larger than that observed from the best metal–metal waveguide devices [6]. This is a result of the larger out-coupling factor for the SI-surface-plasmon waveguide, calculated to be $\alpha_m/(\alpha_m+\alpha_w)=0.6$ (using a mirror loss of $\alpha_m=4.7\ \mathrm{cm}^{-1}$). Although metal–metal waveguides have similar or better values for the scaled waveguide loss α_w/Γ (which determines threshold gain), they exhibit a larger loss α_w (because $\Gamma\sim 1$), and smaller α_m (because of their high facet reflectivity), and thus typically display $\alpha_m/(\alpha_m+\alpha_w)\sim 0.1$. If we consider these calculated loss values, along with an approximate value of $\eta_i=0.5$ for the internal quantum efficiency [6], we find that the measured slope efficiency is still a factor of three less than we might expect. While it is likely that we have underestimated the power somewhat owing to non-ideal collection efficiency, this result suggests that the waveguide losses in the SI-surface-plasmon waveguides may be larger than calculated. This conclusion is bolstered in that, when devices from this wafer were fabricated into metal-metal waveguide ridges (not shown), they exhibited typical thresholds of $J_{th}\sim 370\ \mathrm{A/cm^2}$, which reflects the larger scaled waveguide and mirror losses ($(\alpha_w+\alpha_m)/\Gamma$) in the SI-surface-plasmon waveguides. In any case, improvements in waveguiding, output mode coupling, and reduction in lasing thresholds should enable terahertz QCLs with even higher output powers and efficiencies in the future.

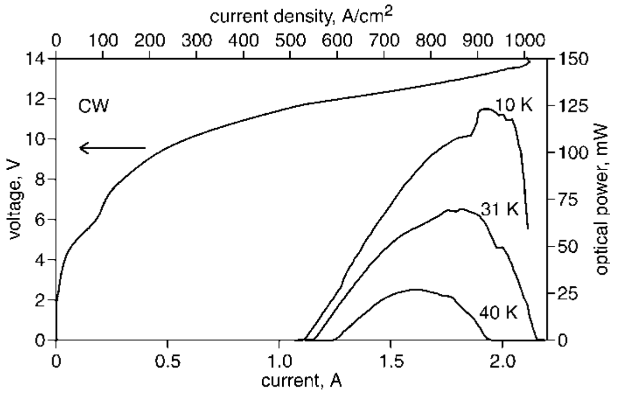

Fig. 3 *Voltage against current at 10 K and collected CW light against current characteristics for HR coated 98 μm × 2.15 mm ridge at various heatsink temperatures*

Acknowledgments: This work is supported by AFOSR, NASA, and NSF. Sandia is a multiprogram laboratory operated by Sandia Corporation, a Lockheed Martin Company, for the US Department of Energy under contract no. DE-AC04-94AL85000.

8 November 2005

Electronics Letters online no: 20063921

doi: 10.1049/el:20063921

B.S. Williams, S. Kumar and Q. Hu (*Department of Electrical Engineering and Computer Science and Research Laboratory of Electronics, Massachusetts Institute of Technology, Cambridge, MA 02139, USA*)

E-mail: bwilliam@mit.edu

J.L. Reno (*Department 1123, Sandia National Laboratories, MS 0601, Albuquerque, NM 87185-0601, USA*)

References

1 Köhler, R., *et al.*: 'Terahertz semiconductor-heterostructure laser', *Nature*, 2002, **417**, pp. 156–159
2 Kumar, S., *et al.*: 2005, unpublished results
3 Barbieri, S.: 2005, Personal communication
4 Gao, J.R., *et al.*: 'Terahertz heterodyne receiver based on a quantum cascade laser and a superconducting bolometer', *Appl. Phys. Lett.*, 2005, **86**, p. 244104
5 Hübers, H.-W., *et al.*: 'Terahertz quantum cascade laser as local oscillator in a heterodyne receiver', *Opt. Express*, 2005, **13**, pp. 5890–5896
6 Williams, B.S., *et al.*: 'Operation of terahertz quantum-cascade lasers at 164 K in pulsed mode and at 117 K in continuous-wave mode', *Opt. Express*, 2005, **13**, pp. 3331–3339
7 Kohen, S., *et al.*: 'Electromagnetic modeling of terahertz quantum cascade laser waveguides and resonators', *J. Appl. Phys.*, 2005, **97**, p. 053106
8 Ajili, L., *et al.*: 'High power quantum cascade lasers operating at $\lambda\approx 87$ and 130 μm', *Appl. Phys. Lett.*, 2004, **85**, pp. 3986–3988
9 Alton, J., *et al.*: 'Optimum resonant tunneling injection and influence of doping density on the performance of THz bound-to-continuum cascade lasers', *Proc. SPIE*, 2005, **5727**, pp. 65–73
10 Williams, B.S., *et al.*: '3.4-THz quantum cascade laser based on longitudinal-optical-phonon scattering for depopulation', *Appl. Phys. Lett.*, 2003, **82**, pp. 1015–1017
11 Lee, A.W.M., and Hu, Q.: 'Real-time, continuous-wave terahertz imaging by use of a microbolometer focal-plane array', *Opt. Lett.*, 2005, **30**, pp. 2563–2565